A microstructure-based constitutive model for cement paste with chemical leaching effect

Wanqing Shen, Jian-Fu Shao, Nicolas Burlion, Z.B. Liu

A microstructure-based constitutive model for cement paste with chemical leaching effect

W.Q. Shen[a,b], J.F. Shao[a,b,*], N. Burlion[b], Z.B. Liu[a]

[a] *Key Laboratory of Ministry of Education on Safe Mining of Deep Metal Mines, College of Resources and Civil Engineering, Northeastern University, Shenyang, 110819, China*
[b] *Univ. Lille, CNRS, Centrale Lille, UMR 9013 - LaMcube - Laboratoire de Mécanique, Multiphysique, Multi-échelle, F-59000 Lille, France*

Abstract

This work focuses on the study of macroscopic mechanical behavior of cement paste in relation with micro-structural degradation due to chemical leaching. According to experimental evidences, the degradation of cement paste is mainly characterized by a significant increase of porosity due to the dissolution of Portlandite (CH) and the decalcification of calcium silicate hydrates (C-S-H). We shall first establish the explicit relations between macroscopic elastic properties and plastic yield stresses and porosity of cement paste by using analytical homogenization methods. With these relations, the degradation of elastic and plastic properties of cement paste by chemical leaching can be systematically determined. Combining with a specific plastic hardening law, the complete micro-macro constitutive model is formulated to describe the mechanical behavior of cement paste under general loading conditions. The efficiency of the proposed model is assessed through the comparison between numerical results and experimental data in uniaxial and triaxial compression tests performed on both sound and leached samples.

Keywords: Cement paste, Concrete, Chemical leaching, Dissolution, Porosity, Homogenization

1. Introduction

In many engineering practices, such as oil and gas exploration, geological disposal of radioactive waste, sequestration of acid gas such CO2 and H2S, cement-based materials

*Corresponding authors: jian-fu.shao@polytech-lille.fr

are widely used as supporting or confining materials. The study of short and long term hydro-mechanical properties of cement-based materials is crucial. For instance, we need to have an in-depth understanding of the evolution of elastic properties, plastic deformation, cracking process, permeability of those materials under complex loading and environmental conditions. Indeed, in many situations, cement-based materials are subjected not only to mechanical loading, but also to moisture transfer, variation of temperature and chemical degradation. The dissolution of Portlandite and the decalcification of CSH are two common processes.

A large number of experimental studies have been devoted to studying basic hydro-mechanical behaviors of cement-based materials under different environmental conditions. It is not planned to provide here an exhaustive synthesis of all those studies. Only some representative studies on effects of physical and chemical degradations on hydro-mechanical properties of cement paste are mentioned. For example, the drying shrinkage deformation and the drying induced effect on mechanical behavior in uniaxial and triaxial compression tests have been investigated in [21]. Some studies have focused on the effect of temperature variation on mechanical strength [1, 6]. Other studies have been performed on different kinds of chemical degradation processes and their effects on mechanical behaviors. The leaching by acid solutions is one of the most frequent processes to be investigated. The degradation of mechanical behavior of cement paste and concrete subjected to chemical leaching under different mechanical loading conditions has been studied [22, 33]. Poro-mechanical properties of leached materials and influences of pore pressure have also been characterized [14]. Some studies have been devoted to the characterization of micro-structure degradation by chemical leaching, in particular the pore structure evolution of cement paste, by using different techniques [15]. Some studies have focused on the calcium leaching process under different values of temperature [7]. A number of studies have been performed on the mechanical and poro-mechanical behaviors of petroleum cement pastes, generally fabricated under specific conditions, under mechanical loading and chemical leaching [10, 34].

Different kinds of studies have also been conducted on modeling of mechanical behavior of cement based materials subjected to chemical leaching. The dissolution of calcium was the principal mechanism considered and described by a phenomenological chemical model giving the relationship between the quantity of dissolved solid calcium and the increase

of porosity [4, 18]. The porosity increase was then interpreted by a macroscopic chemical damage variable. The chemical damage affects both elastic and plastic properties of leached materials [9]. These kinds of models have also been applied to modeling of concrete structures subjected to chemical leaching [16].

However, phenomenological approaches have been used in most previous studies on the modeling of cement-based materials subjected to chemical leaching. The effect of porosity change on the mechanical behavior was generally described by some empirical relations fully identified from limited laboratory tests. The objective of the present study is to provide a theoretical framework to determine the explicit relations between both elastic and plastic properties of cement paste and the variation of porosity by using linear and nonlinear homogenization methods. Based on those theoretical relations, a constitutive model can be formulated for modeling the mechanical behavior of cement paste under general loading conditions and subjected to chemical leaching.

For this purpose, the basic assumption adopted here is that the porosity change is the principal micro-structure evolution induced by the chemical leaching in cement paste. This strong assumption can be relaxed in future extension in order to consider other kinds of micro-structure evolutions. Based on this assumption, it consists in first determining the effective elastic properties and plastic yield criterion of a porous material representing the cement paste. Starting from the pioneer's work by [12], a large number of studies have been conducted on the estimation of effective plastic yield stress or failure stress of different kinds of porous materials by using different kinds of homogenization techniques. For instance, improved effective plastic criteria for ductile failure of porous metal materials have first been developed [23]. In some studies, the effect of pore shape has been taken into account [19, 30]. For geological and cement-based materials, their mechanical behavior generally depends on mean stress and exhibits dissymmetric responses in tension and compression. These specific features have also been considered in porous materials [5, 11, 25, 28, 29].

In spite of all those advances obtained, most existing criteria were mainly applied to materials with small or moderate values of porosity. In order to well describe the plastic behavior of cement paste with high porosity, an improved effective plastic criterion will be adopted. Further, due to the fact that porous cement paste exhibits an important plastic volumetric compaction and a clear brittle-ductile transition behavior, we shall also propose

a non-associative plastic potential and a specific plastic hardening law for the solid cement phase. The present paper is organised as follows: the main mechanical properties of a typical petroleum cement paste subjected to chemical leaching are summarized in section 2. A micromechanics-based elastic plastic model is developed in section 3 including the prediction of effective elastic properties, the effective plastic yield function, the non-associative plastic potential and plastic hardening law. The proposed model is implemented and assessed through numerical simulations and comparisons with experimental data in section 4.

2. Experimental background and basic assumption

The micro-mechanics based model proposed in this paper is strongly based on experimental evidences obtained in previous studies, in particular those reported in [34]. A standard petroleum cement paste with a water-cement (w/c) ratio of 0.44 was investigated. A class G cement and two additives (a dispersing agent and an anti-foam agent) were used to cast the material. The casted samples were first maintained in their mould during 3 days in distilled lime saturated water at 100°C, then removed from their mould and preserved for 4 days more in the distilled lime saturated water at 100°C. After, the temperature was gradually reduced to 90°C (3°C/day) and the samples were kept in the distilled lime saturated water at 90°C to reach a maturation of one month in total. The samples were sliced and rectified under temperature and had a diameter of 37mm and a height of 40mm. The samples were separated into two groups. The first group of samples were placed in a neutral fluid under 90°C (a synthetic fluid which had similar chemical composition to the interstitial fluid). The second one was subjected to chemical leaching with ammonium nitrate (NH4NO3) solution under 90°C until reaching complete degradation state. The concentration of solution was 6mol/l and had a pH value of about 5. The propagation of leached front in samples was determined by using direct observation technique with phenolphthalein solution. The porosity of sound and leached samples was also measured by drying of initially saturated samples at 105°C until constant weight. The leached samples were then rinsed in distilled water before mechanical tests.

Uniaxial and conventional triaxial compression tests were realized respectively on the sound and leached cement paste samples under temperature of 90°C. The axial displacement rate for all tests was 10^{-3} mm/s. The values of confining pressure were 0, 3, 10 and 20MPa.

The initial water permeability of samples was also measured under each value of confining pressure (except for uniaxial compression test). For this purpose, a fluid pressure of 2.5MPa was applied onto the inlet side of samples while the fluid pressure was zero (atmospheric) at the outlet side. After the measurement of permeability, the fluid pressure was set up to a uniform value of 2.5MPa in samples for triaxial tests so that the effective confining pressures are 0.5, 7.5 and 17.5MPa. The neutral fluid was used for the tests on sound samples while the distilled water was used for the tests on leached samples. The loading steps of uniaxial and conventional triaxial compression tests are illustrated in Figure 1.

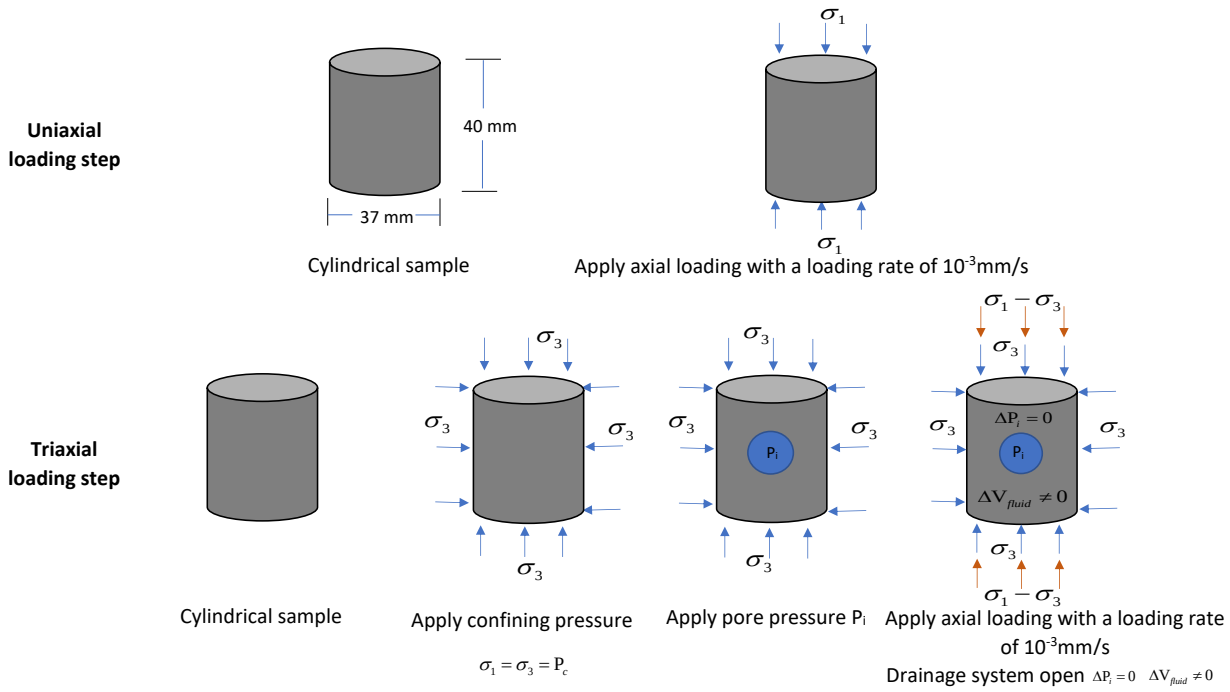

Figure 1: Illustration of loading steps for uniaxial and conventional triaxial compression tests

It was found that the porosity of petroleum cement paste increased from 0.37 at the sound state to 0.57 at the fully leached state. The degradation of the cement paste was mainly due to the dissolution of Portlandite and the decalcification of CSH. The permeability of sound sample at unconfined condition is $2.0 \times 10^{-17} m^2$, which is clearly smaller than that of the chemically degraded one ($4.8 \times 10^{-17} m^2$). This is also due to the significant increase of porosity at the leaching reaction after dissolution of solid calcium. Figure 2 illustrates the

photos of three samples at different states. In Figure 2-a, the samples is not leached and not tested by compression, in Figure 2-b, the samples is not leached but tested under triaxial compression, and in Figure 2-c, the sample is leached and tested in triaxial compression. The effective confining pressure in triaxial compression tests is 7.5 MPa. Comparing with the sound sample in Figure 2-a, the compression tested samples are axially compacted during the loading due to the pore collapse. With the same confining pressure, the compaction of the chemically leached sample is larger than that of the sound one because of its higher porosity generated during the chemical leaching (from 37% to 57%).

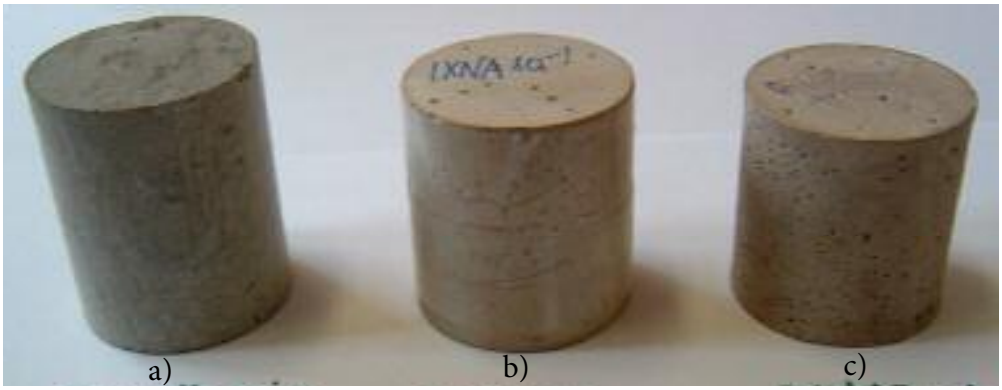

Figure 2: Photography of 3 cement paste samples: (a) sound, (b) sound and tested under triaxial compression at Pc=10 MPa and Pi=2.5 MPa, (c) leached and tested under triaxial compression at Pc=10 MPa and Pi=2.5 MPa.

Due to the leaching process, the uniaxial compression strength (UCS) was reduced by 61% varying from 29MPa to 11MPa. The decrease of compressive strength was well correlated with the increase of porosity. Due to the high porosity even at the sound state (0.37), the basic mechanical behaviour of the oil cement paste was characterized by a small elastic behaviour phase and a very large plastic deformation. The volumetric strain in all mechanical tests was mainly compressive for both the sound and leached samples. As a consequence of this volumetric compaction, there was a clear increase of elastic modulus measured on unloading - reloading cycles during uniaxial and triaxial tests. This increase of elastic modulus was more important in the leached samples than in the sound ones. For the same value of confining pressure, the mechanical behavior of the leached sample was more ductile than that of the sound one. The volumetric strain of samples during the hydrostatic

compression phase (for setting up of desired confining pressure) was also measured. Due to the large increase of porosity induced by the chemical leaching, the volumetric deformability of the leached samples was much higher than that of the sound ones. Plastic deformation occurred in the leached samples as soon as the hydrostatic stress reached 3MPa. For the same values of hydrostatic stress, for instance 3, 10 and 20MPa, the volumetric compacting strains were equal to 0.23%, 0.54% and 1.51% for the sound samples and to 0.53%, 2.88% and 6.68% for the degraded ones. This indicates that a closed plastic yield surface is needed to capture plastic deformation under hydrostatic compression. The stress-strain responses of cement paste in triaxial compression tests were also significantly affected by the chemical leaching. The initial value of elastic modulus (at the beginning of deviatoric loading) was largely reduced by chemical leaching in concordance with the porosity increase. As for most cement-based materials, the initial elastic modulus increased with confining pressure, but this pressure dependency was attenuated in the leached samples. As a consequence of volumetric compaction, the elastic modulus also increased during deviatoric loading. And this increase was much more important in the leached samples than in the sound ones. The initial plastic yield stress and peak stress for all values of confining pressure were strongly reduced by the chemical leaching. As a typical frictional material, the peak deviatoric stress increased with confining pressure. But such an increase was significantly attenuated in the leached samples. As this pressure sensitivity of failure strength is directly related to the frictional coefficient of material, that means that the frictional coefficient of leached samples is clearly lower than that of the sound ones. For instance, by adopting the linear Drucker-Prager criterion to approximate the peak failure stresses obtained, it was found that the cohesion and friction coefficient were reduced by 33% and 63% respectively by the chemical degradation.

Based on these experimental evidences and due to its complex microstructure, as a first approximation, the studied cement paste is treated as a porous medium. The different solid phases of cement paste, such as clinker, CH, high density and low density C-S-H, are mixed and treated as an "equivalent solid matrix" in which the pores are embedded (Figure 3-a). Although this is a strong simplification, it makes it possible to develop an analytical non-linear homogenization procedure and to establish a close-form effective plastic criterion. The variation of porosity due to chemical degradation is one of the key consequences observed in

experimental studies. The principal microstructure degradation of cement paste by chemical leaching is therefore assumed to be the increase of porosity (see Figure 3-b). This can be illustrated by the representative volume element shown in Figure 3. The porosity change of cement paste induces the degradation of elastic and plastic properties of cement paste. Therefore, the main idea of the present study is as follows. We shall first establish the explicit relations between the macroscopic elastic properties and plastic yield stress of cement paste and its porosity, by using analytical linear and nonlinear homogenization methods. With these relations in hand, it will be possible to systematically describe the degradation of elastic and plastic properties with the porosity change due to chemical leaching. We shall then formulate a complete constitutive model by introducing a suitable plastic hardening law in order to describe the mechanical behavior of cement paste in general loading conditions and with the effect of chemical leaching.

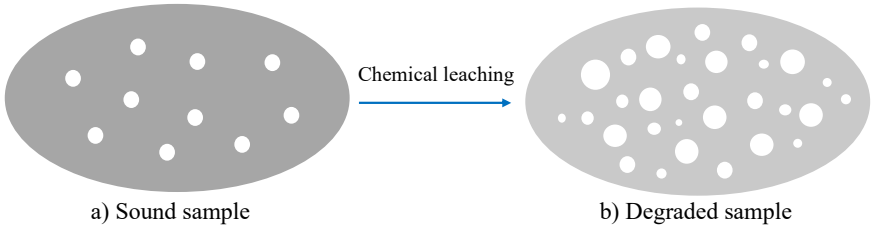

Figure 3: Increase of porosity in cement pase due to chemical leaching process

3. A micro-mechanics-based elastic-plastic model

With the basic assumption adopted above, we shall now determine the effective elastic properties and the effective plastic model for the cement paste.

3.1. Effective elastic behavior

The macroscopic elastic properties of porous cement paste is here determined by using an analytical linear homogenization method. For the sake of simplicity, all pores in the cement paste are assumed to be spherical and randomly distributed in the equivalent matrix phase which is composed of different solid phases. Three homogenization schemes are widely used for the estimation of elastic properties of porous materials: Dilute, Mori-Tanaka and self-consistent schemes. The dilute scheme is suitable for porous materials having a small

volume fraction of pore without interaction. The self-consistent scheme is usually adopted for materials with polycrystalline morphology. There is no dominating phase and each phase can be seen as isolated and embedded in a fictitious effective medium. The Mori-Tanaka scheme is well suitable for materials with a matrix-inclusions (or pores) micro-structure. This is the case for most cement pastes. This scheme allows to account for the interaction between pores in an indirect way. As mentioned above, the porosity of the oil cement paste ranges in $30-60\%$ and the interactions between pores cannot be neglected. Therefore, it seems that the Mori-Tanaka homogenization scheme [20] is the most suitable one for this case. With the assumption of an isotropic solid phase and spherical pores, the effective elastic bulk modulus κ^{eff} and shear modulus μ^{eff} of the cement paste are given by the following relations [2, 35]:

$$\kappa^{eff} = \frac{4(1-f)\kappa_s\mu_s}{4\mu_s + 3f\kappa_s}; \quad \mu^{eff} = \frac{(1-f)\mu_s}{1 + 6f\dfrac{\kappa_s + 2\mu_s}{9\kappa_s + 8\mu_s}} \tag{1}$$

in which κ_s and μ_s denote the elastic bulk and shear moduli of the solid phase (or particles), while f is the porosity of porous paste. According to Figure 3, the total volume of sample is $\mathbf{\Omega}$, the one of the solid phase is denoted as $\mathbf{\Omega}_m$. The corresponding porosity f of the cement paste can be calculated by: $f = \frac{\Omega - \Omega_m}{\Omega}$.

For a given macroscopic strain tensor $\mathbf{D}$ prescribed on the representative volume element (RVE) of cement paste, the corresponding macroscopic stress tensor $\mathbf{\Sigma}$ can be calculated by using the following general elastic relations:

$$\mathbf{\Sigma} = \mathbb{C} : \mathbf{D}, \ \mathbb{C} = 3\kappa^{eff}\mathbb{J} + 2\mu^{eff}\mathbb{K} \tag{2}$$

where $\mathbb{C}$ is the fourth order effective elastic stiffness tensor, $\mathbb{K} = \mathbb{I} - \mathbb{J}$, $\mathbb{I}$ is the fourth-order unity tensor and $\mathbb{J} = \frac{1}{3}\mathbf{1} \otimes \mathbf{1}$, $\mathbf{1}$ is the second-order unity tensor. The expressions of elastic parameters κ^{eff} and μ^{eff} are given in Equation (1) as functions of porosity f and elastic properties of the solid phase (κ_s, μ_s).

3.2. Effective plastic yield criterion

The plastic behavior of porous cement paste is described by the formulation of an effective plastic yield function, a macroscopic plastic potential and a plastic hardening law of the solid phase. As a fundamental difference with classical phenomenological models, the plastic yield

function and potential are explicitly functions of porosity. Further, the effective plastic yield criterion is determined from a nonlinear homogenization procedure. To this end, it is assumed that the plastic yield stress of the solid phase is characterized by the pressure-sensitive Drucker-Prager criterion. It is expressed at the microscopic scale as follows:

$$\Phi(\boldsymbol{\sigma}) = \sigma_{eq} + 3\alpha\sigma_m - \sigma_0 \leq 0 \tag{3}$$

$\boldsymbol{\sigma}$ denotes the local stress field inside the solid phase and $\boldsymbol{\sigma}'$ its deviatoric part, $\sigma_m = \mathrm{tr}\boldsymbol{\sigma}/3$ being the local mean stress and $\sigma_{eq} = \sqrt{\frac{3}{2}\boldsymbol{\sigma}' : \boldsymbol{\sigma}'}$ the local equivalent stress. α and σ_0 are two material parameters, related to the frictional coefficient and the yield stress in the case of purely shearing respectively.

As mentioned above, different forms of effective plastic yield or strength criteria have been proposed for porous materials with a Drucker-Prager type solid phase by using different homogenization techniques. Those criteria are able to consider the effect of porosity and the plastic volumetric strain of the solid phase. A comprehensive comparative study has been presented in [27] between theoretical predictions provided by a variety of existing criteria and numerical results obtained from direct finite element simulations. A large range of porosity and of microscopic frictional coefficient has been considered. Main shortcomings of typical existing criteria have been identified. Based on those comparisons and using a stress-based variational approach with a statically admissible stress field, a new closed form expression of the effective yield criterion has been derived in [27]. That new criterion has brought a significant improvement of theoretical prediction of yield stresses for large values of porosity and for the pure shear loading. Based on this work, the following effective plastic yield criterion is here adopted for the studied porous cement paste:

$$F = \left(\frac{\dfrac{\Sigma_{eq}}{\sigma_0}}{\dfrac{3Z_1}{\sqrt{Z_2}(1-f)} - \dfrac{3\alpha}{1+\gamma\ln(1+sf)}\dfrac{\Sigma_m}{\sigma_0}} \right)^2 + 2f\cosh\left[\frac{sign(\Sigma_m) + 2\alpha}{2\alpha} \ln\left(1 - 3\alpha\frac{\Sigma_m}{\sigma_0}\right) \right] - 1 - f^2 = 0 \tag{4}$$

where Σ_m and Σ_{eq} are the macroscopic mean stress and equivalent one; the parameters Z_1

and Z_2 are functions of porosity f:

$$Z_1 = 1 - \frac{\sqrt{15f}}{25}\sin\left(\frac{\sqrt{15}}{6}\ln(f)\right) - \sqrt{f}\cos\left(\frac{\sqrt{15}}{6}\ln(f)\right), \quad Z_2(f) = 9\frac{1+\frac{11}{25}f-\frac{64}{75}f\ln(f)-2\sqrt{f}T+\frac{34}{375}fU}{1-f},$$

$$U = \sqrt{15}\sin\left(\frac{\sqrt{15}}{3}\ln(f)\right) + 5\cos\left(\frac{\sqrt{15}}{3}\ln(f)\right), \quad T = \frac{\sqrt{15}}{25}\sin\left(\frac{\sqrt{15}}{6}\ln(f)\right) + \cos\left(\frac{\sqrt{15}}{6}\ln(f)\right); \tag{5}$$

$$s = 1 \pm 2\alpha, \quad \gamma = 1 - s^{-1}.$$

This macroscopic yield criterion explicitly depends on the porosity f and the yield properties of equivalent solid phase at the microscopic scale: the frictional parameter α and the pure shearing yield stress σ_0.

As illustrated in Figure 4, the yield surfaces (solid line) predicted by the analytical criterion (4) are compared with the yield stresses given by direct finite element numerical simulations (FEM)(circles) for different values of porosity f and of frictional parameter α. The solid points are the exact solutions of yield stress in the case of hydrostatic loading. More precisely, the results in Figure 4(a) are for the case of $f = 0.2$ with different values of $\alpha = 0$, 0.1, 0.2, 0.25, 0.3 (the corresponding frictional angles are 0, 16.70°, 30.96°, 36.87°, 41.99°). The influence of porosity on the macroscopic yield surface is considered in Figure 4(b) with a constant value $\alpha = 0.2$. With the increase of the frictional parameter α, the macroscopic yield surface increases largely in the compressive domain but decreases slightly in the tensile domain. The dissymmetry of yield stress between compression and tension is thus enhanced. On the other hand, the increase of porosity leads to a significant decrease of the macroscopic yield surface both on the compressive and tensile regions. It is further found that the effective plastic criterion (4) well reproduces the analytical solutions of yield stress for the hydrostatic compression and tension. The values of yield stress in pure shearing when $\frac{\Sigma_{eq}}{\sigma_0}$ are also well predicted for all values of porosity. Therefore, it seems that the influences of porosity and frictional parameter on the overall plastic yield surface are well taken into account by the adopted criterion (4).

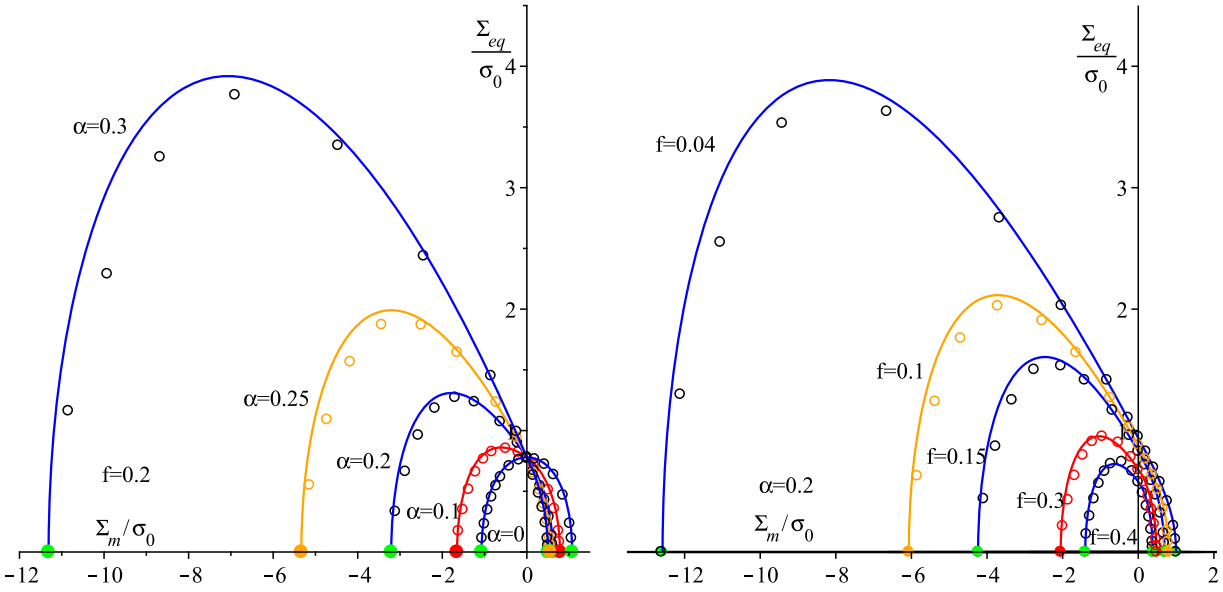

(a) $f = 0.2$ (b) $\alpha = 0.2$

Figure 4: Comparison between plastic yield surfaces predicted by the analytical criterion (4) (solid line) and FEM solutions (open symbols) with different values of frictional parameter α and porosity f; solid points are exact solutions in pure hydrostatic compression and tension

3.3. A complete constitutive elastic-plastic model

As shown by the criterion (4), the macroscopic yield stress is explicitly dependent on the porosity. That means that during plastic deformation of porous materials, plastic volumetric deformation (compaction or dilation) leads to variation of porosity. According, the macroscopic yield stress is also modified. For instance, an increase of porosity generates a decrease of yield stress and then material softening. On the contrary, a decrease of porosity leads to an increase of yield stress and then material hardening. Therefore, the use of the homogenization based plastic criterion (4) implies an intrinsic plastic hardening and softening law due to the evolution of porosity. However, according to previous experimental and numerical studies [3, 13], the porosity evolution alone is generally not enough for capturing complex plastic behavior of highly porous materials. It is found that in addition to porosity change, the local plastic yield stress of the equivalent solid phase also evolves during plastic process due to the fact that this solid phase contains itself different kinds of heterogeneities

at smaller scales. Therefore, some additional laws are needed to capture the plastic hardening of the solid phase. In this study, it is assumed that the shear yield stress of the solid phase σ_0 is a function of an equivalent plastic strain ε^p_{eq}. According to previous studies on porous rocks [13], the following isotropic plastic hardening law is adopted:

$$\bar{\sigma} = \sigma_0^i[1 + a(\varepsilon^p_{eq})^b e^{c\varepsilon^p_{eq}}] \tag{6}$$

in which σ_0^i is the initial value of plastic yield stress $\bar{\sigma}$. a, b and c are three model's parameters defining the evolution of yield stress. The equivalent plastic strain of solid phase ε^p_{eq} will be calculated later.

By substituting the plastic hardening law (6) for the plastic yield criterion (4), one can write the macroscopic plastic yield function as follows:

$$F = \left(\frac{\dfrac{\Sigma_{eq}}{\bar{\sigma}}}{\dfrac{3Z_1}{\sqrt{Z_2}(1-f)} - \dfrac{3\alpha}{1+\gamma\ln(1+sf)}\dfrac{\Sigma_m}{\bar{\sigma}}} \right)^2 + 2f\cosh\left[\frac{sign(\Sigma_m)+2\alpha}{2\alpha}\ln\left(1-3\alpha\frac{\Sigma_m}{\bar{\sigma}}\right)\right] - 1 - f^2 \leq 0 \tag{7}$$

As mentioned in the summary of experimental data, porous cement paste exhibits an important volumetric compaction in deviatoric compression conditions. In order to precisely describe the volumetric deformation of cement paste, it seems that a non-associative plastic flow rule is needed. That means that we shall formulate an independent macroscopic plastic potential for porous cement paste. Compared with the determination of the effective yield criterion (4), the determination of such a plastic potential by a homogenization procedure is mathematically more delicate [17]. A heuristic approach is then adopted [24, 26]. In consists in formulating the macroscopic plastic potential by a simply transformation of the macroscopic plastic criterion. By adopting this approach here, it is assumed that the plastic potential has the same mathematical form as the plastic criterion, but the frictional coefficient of the solid phase α is replaced by another coefficient β. Thus the following macroscopic plastic potential is defined:

$$G = \left(\frac{\dfrac{\Sigma_{eq}}{\bar{\sigma}}}{\dfrac{3Z_1}{\sqrt{Z_2}(1-f)} - \dfrac{3\beta}{1+\gamma\ln(1+sf)}\dfrac{\Sigma_m}{\bar{\sigma}}} \right)^2 + 2f\cosh\left[\frac{sign(\Sigma_m)+2\beta}{2\beta}\ln\left(1-3\beta\frac{\Sigma_m}{\bar{\sigma}}\right)\right] - 1 - f^2 \tag{8}$$

The new parameter β is introduced to better control the plastic volumetric strain and it is conventionally called as the dilatancy coefficient. When $\beta = \alpha$, the associative plastic flow rule is retrieved. It is worth noticing that this macroscopic plastic potential depends also on the porosity and the plastic properties of the solid phase.

With the plastic potential (8) in hand, the macroscopic plastic flow rule is given by:

$$\boldsymbol{D}^p = \dot{\lambda}\frac{\partial G}{\partial \boldsymbol{\Sigma}}(\boldsymbol{\Sigma}; f, \beta, \bar{\sigma}) \tag{9}$$

With the help of the local plastic criterion of solid phase (3) and by using the micro-macro energy equivalence condition: $(1-f)\boldsymbol{\sigma} : \boldsymbol{d}^p = \boldsymbol{\Sigma} : \boldsymbol{D}^p$, the equivalent plastic strain of the solid phase can be calculated:

$$\dot{\varepsilon}^p_{eq} = \frac{\boldsymbol{\Sigma} : \boldsymbol{D}^p}{(1-f)\left[\bar{\sigma} - 3(\alpha-\beta)\frac{\Sigma_m}{(1-f)}\right]} \tag{10}$$

Accordingly, the evolution of porosity is determined with the help of the kinematic compatibility relation:

$$\dot{f} = (1-f)\mathrm{tr}\mathbf{D}^p - \frac{1}{\Omega}\int_{\Omega_m} \mathrm{tr}\boldsymbol{d}^p d\Omega = (1-f)\left[\mathrm{tr}\mathbf{D}^p - 3\beta\dot{\varepsilon}^p_{eq}\right] \tag{11}$$

in which $\boldsymbol{d}^p$ is the local plastic strain rate of the solid phase at the microscopic scale. The plastic multiplier $\dot{\lambda}$ can be determined from the consistency condition:

$$\dot{F}(\boldsymbol{\Sigma}, f, \bar{\sigma}) = \frac{\partial F}{\partial \boldsymbol{\Sigma}} : \dot{\boldsymbol{\Sigma}} + \frac{\partial F}{\partial f}\dot{f} + \frac{\partial F}{\partial \bar{\sigma}}\dot{\bar{\sigma}} = 0 \tag{12}$$

Substituting (6) (10) and (11) for (12), one can get the expression of $\dot{\lambda}$:

$$\begin{aligned}
&\dot{\lambda} = \frac{\dfrac{\partial F}{\partial \boldsymbol{\Sigma}} : \mathbb{C} : \mathbf{D}}{H^G}, \quad \text{with} \\
&H^G = \frac{\partial F}{\partial \boldsymbol{\Sigma}} : \mathbb{C} : \frac{\partial G}{\partial \boldsymbol{\Sigma}} - \frac{\partial F}{\partial f}\left[(1-f)\frac{\partial F}{\partial \Sigma_m} - 3\beta\frac{\boldsymbol{\Sigma} : \dfrac{\partial G}{\partial \boldsymbol{\Sigma}}}{\bar{\sigma} - 3(\alpha-\beta)\frac{\Sigma_m}{1-f}}\right] - \frac{\partial F}{\partial \bar{\sigma}}\frac{\partial \bar{\sigma}}{\partial \varepsilon^p_{eq}}\frac{\boldsymbol{\Sigma} : \dfrac{\partial G}{\partial \boldsymbol{\Sigma}}}{\bar{\sigma} - 3(\alpha-\beta)\frac{\Sigma_m}{1-f}}
\end{aligned} \tag{13}$$

By using the value of $\dot{\lambda}$, the incremental form of elastic-plastic constitutive relations can be written as $\dot{\boldsymbol{\Sigma}} = \mathbb{L} : \dot{\mathbf{D}}$. The tangent elastic-plastic operator can be determined as follows:

$$\mathbb{L} = \begin{cases} \mathbb{C} & \text{if} \quad F \leq 0, \dot{F} < 0 \\ \mathbb{C} - \dfrac{\left(\mathbb{C} : \frac{\partial F}{\partial \boldsymbol{\Sigma}}\right) \otimes \left(\frac{\partial F}{\partial \boldsymbol{\Sigma}} : \mathbb{C}\right)}{H^G} & \text{if} \quad F = 0, \dot{F} > 0 \end{cases} \tag{14}$$

The micro-mechanics-based constitutive model presented above is implemented in the standard finite element code (Abaqus software) by using a user subroutine UMAT for the numerical simulation of a material point. The standard elastic predictor - plastic corrector operator split algorithm is used. The efficiency of the proposed model will be assessed in the following section.

4. Numerical assessment and experimental validation

As mentioned above, the main microstructure evolution of cement paste due to the chemical leaching is the increase of porosity by the dissolution of solid calcium. The solid phase of cement paste exhibits a plastic hardening. The numerical response of the proposed model is here assessed by a sensitivity study of main parameters controlling those two chemical and mechanical mechanisms. The performance of the model is further verified through comparisons with experimental data.

4.1. Sensitive study of main parameters

In our micro-macro model, there are two elastic parameters (Young's modulus E_s and Poisson's ratio ν_s) and four parameters for plastic hardening of the solid phase (σ_0^i, a, b and c), as well as the frictional and dilatancy coefficients (α and β) of the solid phase. The macroscopic behavior is further inherently influenced by the porosity f which describes the evolution of microstructure. To get a clear idea on the dependency of macroscopic responses on microscopic parameters, a sensitivity study is helpful. For this purpose, a reference set of parameters is selected and given in Table 1 for the sensitive study. The initial porosity of sound cement paste is $f = 0.37$ which is chosen as the reference.

Young's modulus E_s	Poisson's ratio ν_s	Frictional parameter α	Dilatancy parameter β	Plastic hardening parameters σ_0^i	a	b	c
16GPa	0.2	0.23	0.015	1 MPa	100	0.16	2.5

Table 1: Reference set of parameters for the cement paste with a non-associative flow rule

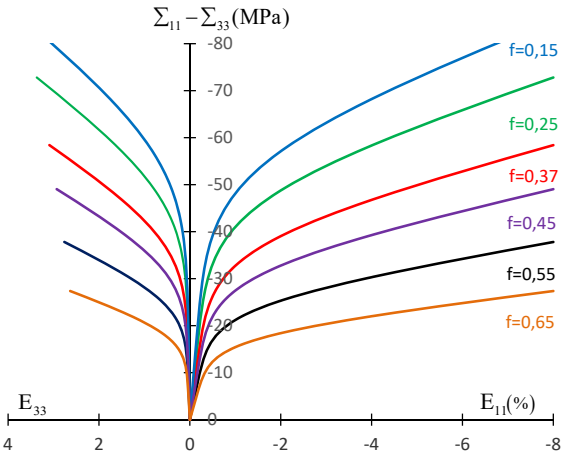

(a) Effect of porosity f, P_c=0

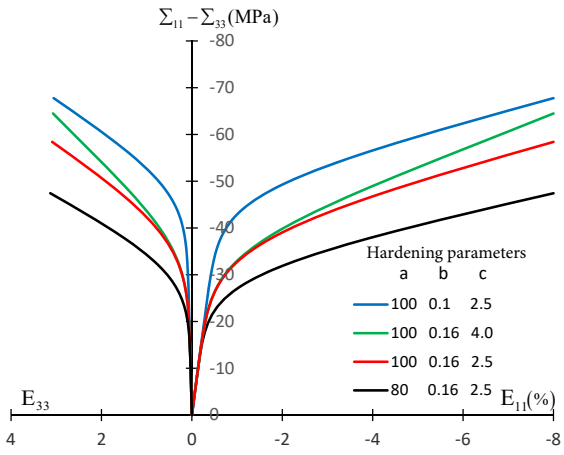

(b) Hardening parameter a, b, c, P_c=0

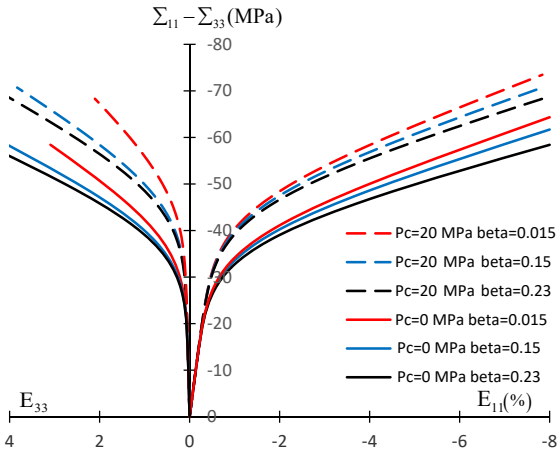

(c) Dilatancy parameter β, α = 0.23

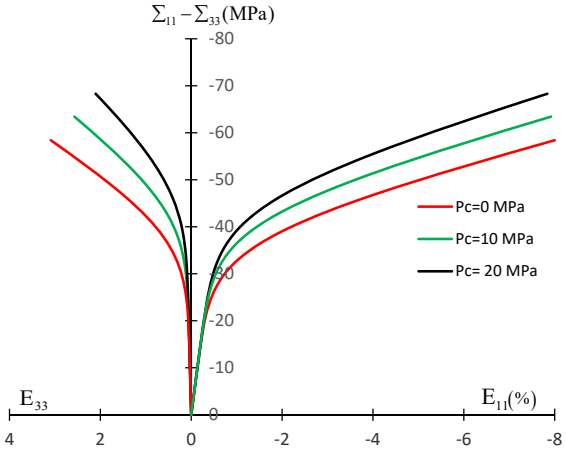

(d) Influence of confining pressure

Figure 5: Influence of model's parameters on the macroscopic behavior of cement paste

A series of uniaxial and triaxial compression tests are simulated with the proposed model. The results obtained with the reference set of parameters are represented by the red lines in all Figures. The macroscopic stress-strain curves in uniaxial compression test are shown in Figure 5(a) for different values of initial porosity in the range of $f = 0.15 \sim 0.65$. It is clear that the macroscopic mechanical behavior of cement paste is strongly affected by the initial value of porosity. With the increase of porosity, the macroscopic elastic modulus, initial plastic yield stress and failure strength are drastically reduced. These results are qualitatively in agreement with most experimental data reported on porous materials. The sensitivity of macroscopic response in uniaxial compression test to three plastic hardening

parameters a, b and c is shown in Figure 5(b). One can see that the parameters a and b mainly control the plastic hardening rate at the first stage of loading when the accumulated plastic strain is still small, while the parameter c has an important effect on the plastic hardening rate in a subsequent stage when the plastic strain becomes large. With the increase of a or the decrease of b, the plastic hardening rate is enhanced. From Figure 5(c), one can see that the dilatancy parameter β not only affects the lateral strain, but also has a little influence on the plastic hardening rate. The stress-strain curves in triaxial compression tests with different confining pressures (0 MPa, 10 MPa and 20 MPa) are presented in Figure 5(d). The classical effect of confining pressure on mechanical behavior of frictional materials is well reproduced by the micro-macro model.

4.2. Experimental verification

In this section, the proposed microstructure-based elastic-plastic model is verified against the experimental data obtained on the cement paste reported in [34]. As mentioned in section 2, the initial porosity f of the sound samples is about 37% and that of the completely leached ones is about 57%. Uniaxial and triaxial compression tests have been performed respectively on the sound and leached samples. These tests are simulated with the proposed micro-macro model by considering the variation of porosity. The general strategy for the determination of the model's parameters is as follows: based on the stress-strain relation of the conventional triaxial compression test of sound sample at an effective confining pressure 17.5 MPa, the elastic and plastic behavior can be determined. With the macroscopic elastic properties (κ^{eff}, μ^{eff}) obtained from the experiment, the parameters of the equivalent matrix phase can be calculated by the inverse procedure with Equation (1) and the corresponding porosity $f = 0.37$. Concerning the plastic parameter, an iterative procedure is adopted. Based on the sensitive studies of model's parameters, the values of plastic parameters of the equivalent matrix phase can be optimized in an iterative way by comparing numerical results and experimental data. The obtained parameters are then used in the simulations of other tests performed on different confining pressures. The identified values are given in Table 1. The basic idea is that all the mechanical parameters are remained the same for both the sound and leached samples. Only the value of porosity is changed. This marks the key difference with most phenomenological models for which empirical relations are used to

capture evolutions of mechanical parameters with porosity. As indicated in [8, 31, 32], it is interesting to relate the model prediction of macroscopic mechanical properties directly to the original compositions of the studied material and takes into account automatically their evolutions, but a more complex yield criterion are needed which considers fully the microstructure information.

For instance, based on the Young's modulus and Poisson's ratio of the equivalent solid phase and the porosity f, the macroscopic elastic bulk modulus κ^{eff} and shear modulus μ^{eff} of the porous cement paste can be calculated according to the relations (1). The variations of κ^{eff} and μ^{eff} of the cement paste are shown in Figure 6 as a function of porosity variation Δf during the chemical leaching process. The experimental values of bulk and shear moduli obtained from triaxial compression tests on the sound and completely leached samples are also reported on this Figure (symbols). It is clear that the elastic properties of cement paste are significantly reduced by the chemical leaching and the theoretical predictions agree well with the experimental data.

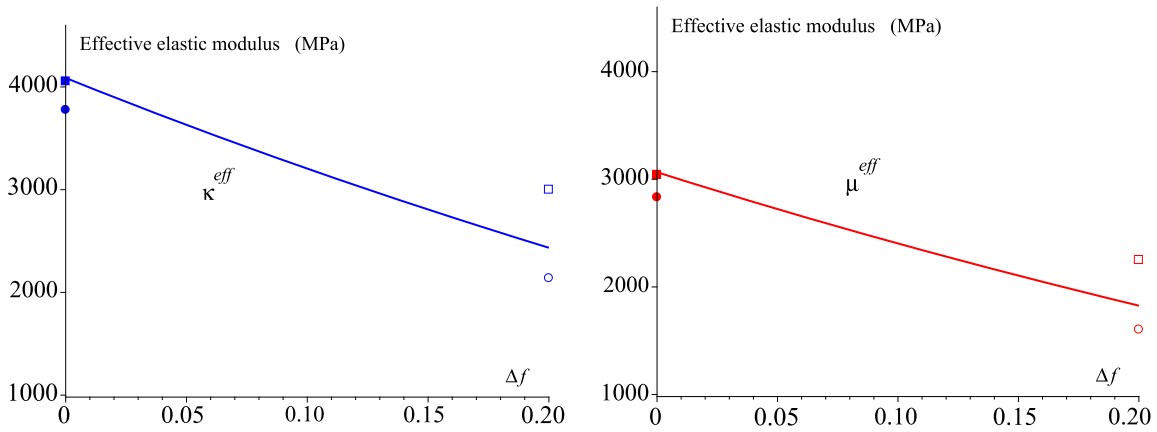

(a) bulk modulus

(b) shear modulus

Figure 6: Evolution of the effective elastic bulk modulus κ^{eff} and shear modulus μ^{eff} of cement paste as a function of porosity variation: comparison between theoretical predictions (lines) and experimental measurements (symbols).

The plastic and failure behavior is also sensitive to chemical leaching. In order to show the effect of chemical leaching on the macroscopic failure behavior, we shall here investigate

the evolution of the uniaxial compressive strength (R_c) as a function of porosity variation Δf at different levels of plastic hardening, i.e. for different values of the shear yield stress of solid phase $\bar{\sigma}$ in the relation (6). The obtained results are given in Figure 7(a). It is obvious that the increase of porosity f due to chemical leaching leads to a significant reduction of mechanical strength. It is worth noticing that due to plastic hardening, the solid phase is hardened. But it is interesting to observe that the degradation rate of compressive strength R_c with the porosity increase is higher for the hardened solid phase than for the softer one.

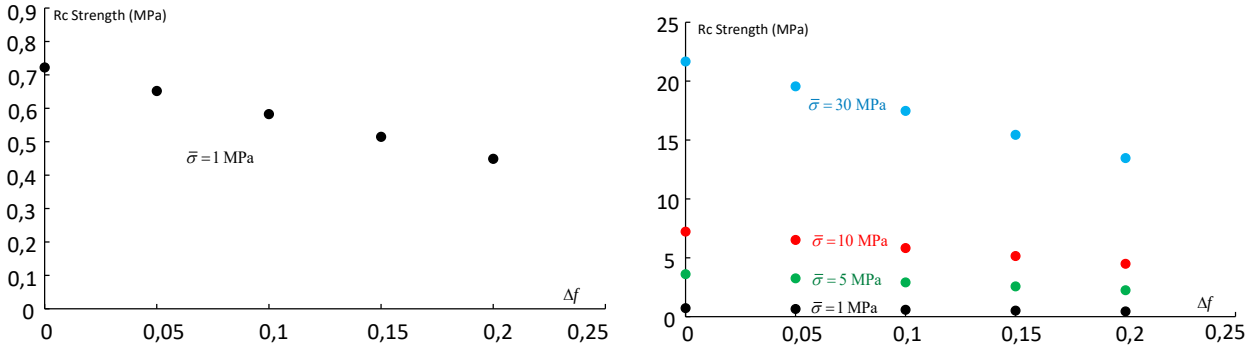

(a) $\bar{\sigma}$ = 1 MPa

(b) $\bar{\sigma}$ = 5, 10, 30 MPa

Figure 7: Degradation of uniaxial compression strength of cement paste as a function of variation of porosity Δf for different levels of plastic hardening of solid phase.

The macroscopic stress-strain curves for triaxial compression tests under different values of effective confining pressure (0 MPa, 7.5 MPa and 17.5 MPa) are now presented in Figure 8-10. Numerical results given with the micro-macro model (continuous lines) are compared with experimental data (empty circles), for both the sound and completely leached samples. It is recalled that the same values of elastic and plastic parameters should be used for the two groups of samples and only the porosity is increased from 37% to 57%. However, it is found that the mechanical behavior of leached samples becomes more ductile (smooth peak stress) than that of sound ones. This is characterized by a lower plastic hardening rate. It seems that the plastic hardening kinetics should vary with porosity variation. A detailed description of this phenomenon requires experimental data obtained on partially leached samples. In the absence of such data and as a first approximation, a lower value of the hardening parameter $a_{degra} = 60$ is here used for the leached samples. As illustrated in Figure 8-10, a general good

agreement is found between the numerical results and experimental data. The influence of chemical degradation on the mechanical behavior of cement paste seems to be well taken into account. In Figures 11 and 12, one shows the evolutions of porosity f as a function of axial strain during triaxial compression tests for both the sound and degraded samples. In all cases, there is a decrease of porosity during deviatoric loading $\Sigma_{11} - \Sigma_{33}$. This decrease of porosity is due to the plastic volumetric compaction. However, the porosity decrease remains moderate compared with the porosity change induced by the chemical leaching process.

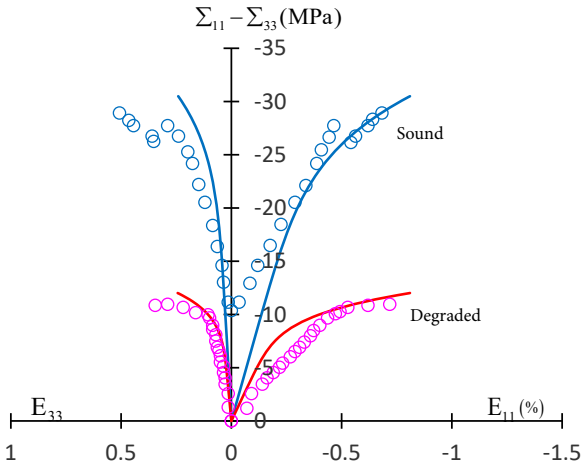

Figure 8: Comparison between the numerical predictions (lines) and experimental data (circles) for sound and degraded samples, uniaxial compression test Pc = 0 MPa.

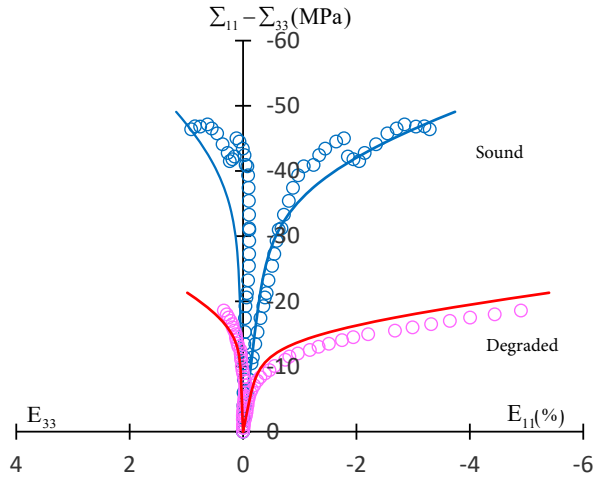

Figure 9: Comparison between the numerical predictions (lines) and experimental data (circles) for sound and degraded samples, confining pressure Pc = 7.5 MPa.

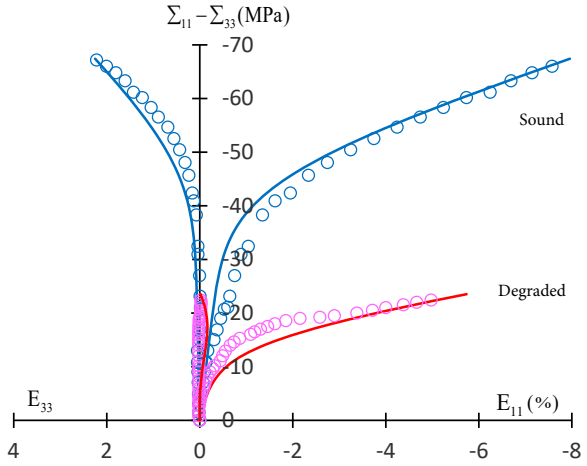

Figure 10: Comparison between the numerical predictions (lines) and experimental data (circles) for sound and degraded samples, confining pressure Pc = 17.5 MPa.

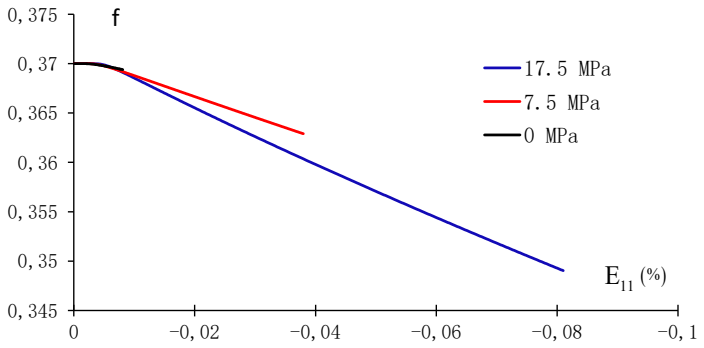

Figure 11: Evolution of porosity f as a function of axial strain in the sound samples with different confining pressures.

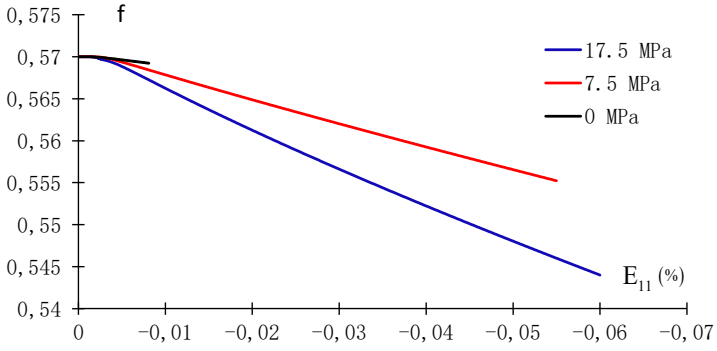

Figure 12: Evolution of porosity f as a function of axial strain in the degraded samples with different confining pressures.

In Figure 13, we present the peak deviatoric stresses of the cement paste for different values of mean stress. The numerical results (empty squares) are compared with experimental values (plain rhombus) for both the sound (blue) and degraded (red) samples. It is noted that for triaxial compression tests under a high confining pressure, no peak deviatoric stress is obtained until the end of test (stopped due to the limitation of strain measurement instrument). The values reported here are taken for a large value of axial strain reached during the test. According to these comparisons, it is found that the proposed micro-mechanics based model well describes the macroscopic failure surface of both sound and leached cement paste samples.

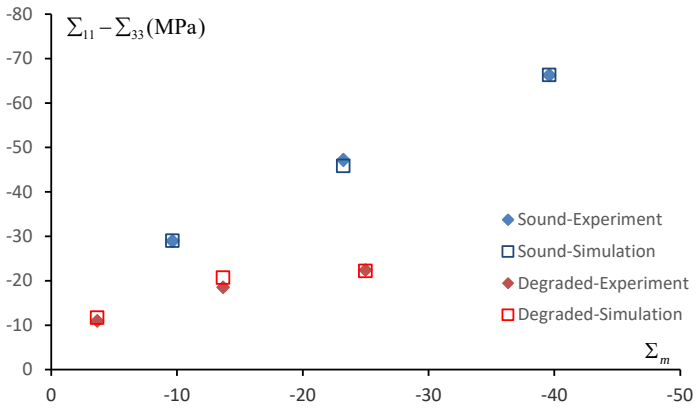

Figure 13: Comparison of failure deviatoric stress between experimental data and numerical results for the sound and degraded samples.

5. Conclusions

The chemical leaching of cement paste leads to a significant increase of porosity. The macroscopic mechanical behavior of cement paste is strongly influenced by the porosity variation. Based on this assumption, we have proposed a micro-mechanics-based elastic-plastic model to describe the mechanical behavior of cement paste under general loading conditions and subjected to chemical leaching. The macroscopic elastic properties are expressed as functions of porosity. An analytical form of macroscopic plastic yield criterion has been determined by using a nonlinear homogenization technique. The plastic hardening of solid phase in cement paste has also been taken into account. A macroscopic plastic potential has been formulated to define a non-associative plastic flow rule. The complete constitutive model is implemented into a standard finite element computing code. The proposed model is able to describe the main features of mechanical behavior of porous cement paste, such as pressure dependency of yield stress, plastic deformation under hydrostatic compression and tension, strong dissymmetry of response between compression and tension, plastic volumetric compaction and dilatancy. Most importantly, compared with most phenomenological models, the micro-mechanics based model is able to explicitly describe the degradation of both elastic and plastic properties of cement paste due to chemical leaching, without introducing empirical laws fitted from laboratory tests. The numerical results provided by the proposed model for triaxial compression tests on the oil cement paste are in good agreement

with the experimental data. Together with a suitable chemical dissolution model, the proposed model can be used to solve boundary values problems of concrete structures subjected to both mechanical loads and chemical leaching.

Acknowledgement

This study was partially supported by the National Natural Science Foundation of China (Grant No. 11902069).

References

[1] Bahafid, S., Ghabezloo, S., Faure, P., Duc, M., Sulem, J., 2018. Effect of the hydration temperature on the pore structure of cement paste: Experimental investigation and micromechanical modelling. Cement and Concrete Research 111, 1 – 14.

[2] Bornert, M., Bretheau, T., Gilormini, P., 2001. Homogeneisation en mecanique des materiaux 1. materiaux aleatoires elastiques et milieux periodiques.

[3] Burlion, N., Bernard, D., Chen, D., 2006. X-ray microtomography: Application to microstructure analysis of a cementitious material during leaching process. Cement and Concrete Research 36 (2), 346 – 357.

[4] Carde, C., Francois, R., Torrenti, J., 1996. Leaching of both calcium hydroxide and c-s-h from cement paste: modelling the mechanical behavior. Cem. Conc. Res. 26, 1257–1268.

[5] Cazacu, O., Stewart, J. B., 2009. Analytic plastic potential for porous aggregates with matrix exhibiting tension-compression asymmetry. Journal of the Mechanics and Physics of Solids 57, 325–341.

[6] Chari, M. N., Shekarchi, M., Sobhani, J., Chari, M. N., 2016. The effect of temperature on the moisture transfer coefficient of cement-based mortars: An experimental investigation. Construction and Building Materials 102, 306 – 317.

[7] de Larrard, T., Benboudjema, F., Colliat, J., Torrenti, J., Deleruyelle, F., 2010. Concrete calcium leaching at variable temperature: Experimental data and numerical model inverse identification. Computational Materials Science 49 (1), 35 – 45.

[8] Geng, G., Myers, R., Qomi, M. e. a., 2017. Densification of the interlayer spacing governs the nanomechanical properties of calcium-silicate-hydrate. Sci Rep 7, 10986.

[9] Gerard, B., Pijaudier-Cabot, G., Laborderie, C., 1998. Coupled diffusion-damage modelling and the implications on failure due to strain localisation. Int. J. Solids Struct. 35, 4107–4120.

[10] Ghabezloo, S., Sulem, J., Guedon, S., Martineau, F., Saint-Marc, J., 2008. Poromechanical behaviour of hardened cement paste under isotropic loading. Cem. Conc. Res. 38, 1424–1437.

[11] Guo, T., Faleskog, J., Shih, C., 2008. Continuum modeling of a porous solid with pressure sensitive dilatant matrix. J. Mech. Phys. Solids 56, 2188–2212.

[12] Gurson, A., 1977. Continuum theory of ductile rupture by void nucleation and growth: Part I-yield criteria and flow rules for porous ductile media. J. Engrg. Mater. Technol. 99, 2–15.

[13] Han, B., Shen, W., Xie, S., Shao, J., 2020. Plastic modeling of porous rocks in drained and undrained conditions. Computers and Geotechnics 117, https://doi.org/10.1016/j.compgeo.2019.103277.

[14] Heukamp, F., Ulm, F., Germaine, J., 2003. Poroplastic propreties of calcium-leached cement based materials. Cem. Conc. Res. 33, 1155–1173.

[15] Kjellsen, K., Detwiler, R., Gjorv, O., 1991. Development of microstructures in plan cement pastes hydrated at different temperatures. Cem. Conc. Res. 21, 179–189.

[16] LeBellego, C., Gerard, B., Pijaudier-Cabot, G., 2000. Chemo-mechanical effects in mortar beams subjected to water hydrolysis. ASCE J. Eng. Mech. 126, 266–272.

[17] Maghous, S., Dormieux, L., Barthelemy, J., 2009. Micromechanical approach to the strength properties of frictional geomaterials. European Journal of Mechanics A/Solid 28, 179–188.

[18] Mainguy, M., Tognazzi, C., Torrenti, J., Adenot, F., 2000. Modelling of leachinfg in pure cement paste and mortar. Cem. Conc. Res. 30, 83–90.

[19] Monchiet, V., Charkaluk, E., Kondo, D., 2014. Macroscopic yield criteria for ductile materials containing spheroidal voids: An eshelby-like velocity fields approach. Mechanics of Materials 72, 1–18.

[20] Mori, T., Tanaka, K., 1973. Average stress in a matrix and average elastic energy of materials with misfitting inclusions. Acta Metall.Mater 42(7), 597–629.

[21] Neubauer, C., Jennings, H., Garboczi, E., 1997. Mapping drying shrinkage deformations in cement-based materials. Cement and Concrete Research 27 (10), 1603 – 1612, materials Research Society Symposium on Structure-Property Relationships in Hardened Cement Paste and Composites.

[22] Nguyen, V., Colina, H., Torrenti, J., Boulay, C., Nedjar, B., 2007. Chemo-mechanical coupling behaviour of leached concrete part i: Experimental results. Nucl. Eng. Des. 237, 2083–2089.

[23] Pardoen, T., Hutchinson, J., 2003. Micromechanics-based model for trends in toughness of ductile metals. Acta Mater 51, 133–148.

[24] Shen, W., Kondo, D., Dormieux, L., Shao, J., 2013. A closed-form three scale model for ductile rocks with a plastically compressible porous matrix. Mechanics of Materials 59, 73–86.

[25] Shen, W., Oueslati, A., De Saxce, G., 2015. Macroscopic criterion for ductile porous materials based on a statically admissible microscopic stress field. International Journal of Plasticity 70, 60–76.

[26] Shen, W., Shao, J., Kondo, D., Gatmiri, B., 2012. A micro-macro model for clayey rocks with a plastic compressible porous matrix. International Journal of Plasticity 36, 64–85.

[27] Shen, W., Shao, J., Liu, Z., Oueslati, A., Saxcé, G. D., 2020. Evaluation and improvement of macroscopic yield criteria of porous media having a drucker-prager matrix. International Journal of Plasticity 126, 102609.

[28] Shen, W., Shao, J., Oueslati, A., Saxcé, G. D., Zhang, J., 2018. An approximate strength criterion of

porous materials with a pressure sensitive and tension-compression asymmetry matrix. International Journal of Engineering Science 132, 1–15.

[29] Shen, W. Q., Shao, J. F., Kondo, D., De Saxce, G., 2015. A new macroscopic criterion of porous materials with a mises-schleicher compressible matrix. European Journal of Mechanics A/Solids 49, 531–538.

[30] Shen, W. Q., Zhang, J., Shao, J. F., Kondo, D., 2017. Approximate macroscopic yield criteria for drucker-prager type solids with spheroidal voids. International Journal of Plasticity 99, 221–247.

[31] Thomas, J. J., Chen, J. J., Allen, A. J., Jennings, H. M., 2004. Effects of decalcification on the microstructure and surface area of cement and tricalcium silicate pastes. Cement and Concrete Research 34 (12), 2297 – 2307.

[32] Wyrzykowski, M., Sanahuja, J., Charpin, L. e. a., 2017. Numerical benchmark campaign of cost action tu1404 - microstructural modelling. RILEM Technical Letters 2, 99–107.

[33] Xie, S., Shao, J., Burlion, N., Saint-Marc, J., Garnier, A., 2008. Experimental study of mechanical behaviour of cement paste under compressive stress and chemical degradation. Cement and Concrete Research 38, 1416–1423.

[34] Yurtdas, I., Xie, S., Burlion, N., Shao, J., Saint-Marc, J., Garnier, A., 2011. Influence of chemical degradation on mechanical behavior of a petroleum cement paste. Cement and Concrete Research 41(4), 412–421.

[35] Zaoui, A., 2000. Materiaux heterogenes et composite.